SCIENCE CHINA
Chemistry

•ARTICLES•

July 2020 Vol.63 No.7: 1012–1018
https://doi.org/10.1007/s11426-020-9717-8

CuO/Cu_2O nanowire array photoelectrochemical biosensor for ultrasensitive detection of tyrosinase

Xiaoxi Guo[1], Jinghua Wu[1], Lian Xia[1], Meihao Xiang[1], Fengli Qu[1*] & Jinghong Li[2]

[1]*College of Chemistry and Chemical Engineering, Qufu Normal University, Qufu 273165, China;*
[2]*Department of Chemistry, Key Laboratory of Bioorganic Phosphorus Chemistry & Chemical Biology, Tsinghua University, Beijing 100084, China*

Received February 3, 2020; accepted March 5, 2020; published online April 1, 2020

Photoelectrochemical (PEC) biosensors have shown great promise in bioanalysis and diagnostic applications in recent years. In this work, the CuO/Cu_2O nanowire array (CuO/Cu_2O Nanowire) supported on copper foam was prepared as a photocathode for detection of tyrosinase though quinone-chitosan conjugation chemistry method. The *in-situ* generated quinones that were the catalytic product of tyrosinase acted as electron acceptors, which were captured by the chitosan deposited on the surface of the electrode. Direct immobilization of electron acceptor on the electrode surface improved the photocurrent conversion efficiency and thus sensitivity. The as-prepared biosensor can realize a rapid response in a wide linear range of 0.05 U/mL to 10 U/mL with the detection limit as low as 0.016 U/mL of tyrosinase. The current work provides a new perspective to design and develop highly sensitive and selective PEC biosensor.

tyrosinase, CuO/Cu_2O nanowire, photoelectrochemical biosensor, chitosan modified electrode, quinones

Citation: Guo X, Wu J, Xia L, Xiang M, Qu F, Li J. CuO/Cu_2O nanowire array photoelectrochemical biosensor for ultrasensitive detection of tyrosinase. *Sci China Chem*, 2020, 63: 1012–1018, https://doi.org/10.1007/s11426-020-9717-8

1 Introduction

Tyrosinase, as a binuclear copper-containing enzyme, is widely distributed in all kinds of organism, such as plants, animals and microorganism [1–4]. The enzyme can catalyze two sequential reactions: the hydroxylation of phenolic substrates to catechol derivatives, and subsequently oxidation catechol derivatives to orthoquinone products [5–7]. Tyrosinase activity is vital to biosynthesis of melanin, which is critical for skin color [8,9]. More importantly, it can catalyze the dopamine, which is a neurotransmitter in the mammalian central nervous system [10]. In addition, it is also a key factor in the nutritional value of fruits and vegetables [11]. The disruption of tyrosinase is thought to be associated with melanoma cancer, skin and Parkinson's diseases. Accordingly, developing a sensitive and selective method to detect tyrosinase activity is highly essential for both clinical diagnosis and the food industry.

In the past few years, lots of techniques have been reported for detection of tyrosinase, such as colorimetric method [12,13], electrochemical method [14,15] and fluorescence method [16,17]. But those approaches suffer from low sensitivity, poor repeatability, time-consuming modifying process, etc., which limits their practical applications. Photoelectrochemical (PEC) method that combines photochemical process and electrochemical technology possesses the inherit advantages including simple instrumentation, fast detection process and easy of miniaturization. Thus, it has been widely employed for detection of various analytes. Many reported biosensors change the PEC signals by *in-situ* producing electron donor or acceptor in electrolyte. In recent years, Zhao *et al.* [18] used alkaline phosphatase to catalyze

*Corresponding author (email: qflhn@126.com)

the hydrolysis of ascorbic acid 2-phosphate to *in-situ* produce ascorbic acid for efficient electron donating. Wang *et al.* [19] employed the DNAzyme catalyzed oxidation of hydroquinone to *in-situ* generate the electron acceptor. However, the low concentration of the electron donor or acceptor reduces the chance of colliding with electrode surface, which leads to decreased sensitivity.

Photoactive materials are significant parts of the PEC system. Since the visible light can reduce the damage to analytes, the visible-light PEC materials are widely investigated. To enhance the absorption efficiency of the visible light, the heterojunction materials have been developed as promising alternatives, which consist of two or even more phases with different band gaps [20–23]. Such heterojunction materials can broaden the light absorption edge to the visible region and meanwhile possess high transfer efficiency of photogenerated charges [24–26]. It is well-accepted that CuO and Cu_2O possess outstanding properties such as high abundance, low cost, facile fabrication, and nontoxicity. Therefore, the combination of CuO and Cu_2O to form heterojunction materials will improve the stability, and facilitate the charge separation and the absorption efficiency of the visible light. In addition, three dimension (3D) structure has large surface area, high active sites density, low series resistance, marvelous stability and beneficial diffusion of electrolyte, which is beneficial for sensitivity [27,28].

Herein, we report the CuO/Cu_2O nanowire array (CuO/Cu_2O Nanowire) supported on copper foam as photocathode for detection of tyrosinase through quinone-chitosan conjugation chemistry method [29]. As exhibited in Scheme 1, the 3D electrode was decorated by chitosan and the surface of CuO/Cu_2O Nanowire contained a large amount of amino group. The tyrosine and tyrosinase were incubated together to *in-situ* generate quinones which were used as electron acceptors. Then, the CuO/Cu_2O Nanowires were immersed in the mixture to capture the quinones by quinone-chitosan conjugation chemistry method. In this process, the generated quinones can undergo two different reactions with the amino group on the chitosan through Schiff bases or/and Michael-type adducts [30]. During the illumination process, the electrons on valence bands of both Cu_2O and CuO are excited to their conductive bands, resulting in the holes on their valence bands. The excited electrons on conductive band of Cu_2O are injected to that of CuO and consumed by the quinones immediately. The holes on the valence band of CuO are transferred to that of Cu_2O and scavenged by the electrons from conductive copper foam. In such process, the quinones immobilized on electrode surface will efficiently capture the electrons and thus improve the sensitivity of the biosensor. The proposed biosensor can realize a rapid response in a wide linear range of 0.05 U/mL to 10 U/mL with the detection limit as low as 0.016 U/mL.

2 Experimental

2.1 Materials and reagents

Tyrosinase was purchased from Sangon Biotech Co., Ltd. (Shanghai, China). Tyrosine and chitosan were brought from Sigma-Aldrich (St. Louis, MO, USA). 4-benzoquinone, $(NH_4)_2S_2O_8$ and NaOH were obtained from Aladdin Industrial Corporation (Shanghai, China). The copper foam was supplied by Changsha Liyuan New Material Ltd. Human serum samples were gathered from the Qufu Normal University Hospital. All experiments were carried out in accordance with the guidelines of the National Institute of Health, China, and approved by the Institutional Ethical Committee (IEC) of Qufu Normal University. We also obtained informed consent for any experimentation with human serum samples. All stock solutions were prepared with deionized water. All reagents were used as received. The water employed throughout the experiments was deionized water.

2.2 Characterization methods

All the electrochemical measurements were performed by a

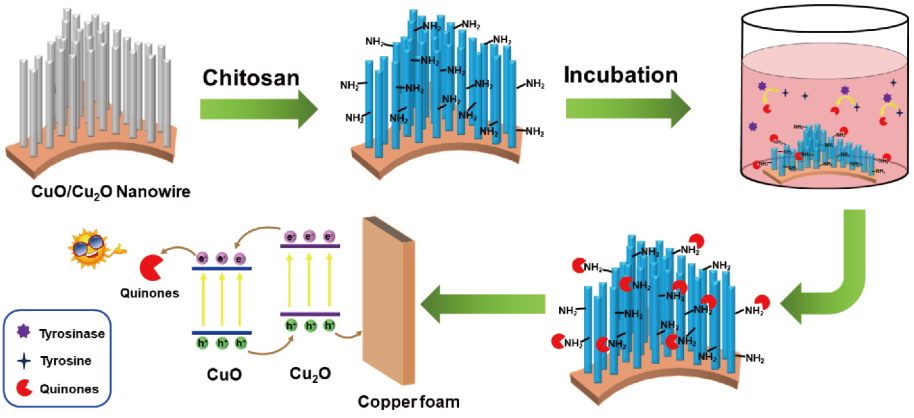

Scheme 1 Schematic illustration for the process to synthesize the CuO/Cu_2O Nanowire and fabricate the PEC sensor for tyrosinase detection and the mechanism of the operating PEC system (color online).

CHI 760E electrochemical workstation (CH Instruments, Inc., Shanghai, China) in a typical three electrode configuration, CuO/Cu_2O Nanowire (0.5 cm×0.5 cm) as the working electrode, a saturated calomel electrode (SCE) as the reference electrode and a platinum wire as the auxiliary electrode. Powder X-ray diffraction (XRD) patterns were acquired on a LabX XRD-6100 X-ray diffractometer (SHIMADZU, Japan) with Cu Kα radiation (40 kV, 30 mA) of wavelength 0.154 nm. Fourier transform infrared (FTIR) absorption spectra were determined using FTIR (iD7 ATR Nicolet iS5 Spectrometer, Thermo Fisher, USA). Scanning electron microscopy (SEM) measurements were performed on a tungsten lamp-equipped SU3500 scanning electron microscope (HITACHI, Japan) at an accelerating voltage of 2 kV. Transmission electron microscopy (TEM) measurements were conducted on a Hitachi H-8100 electron microscopy (Hitachi, Tokyo, Japan) at an accelerating voltage of 200 kV. X-ray photoelectron spectroscopy (XPS) measurements were carried out on an ESCALABMK II X-ray photoelectron spectrometer using Mg as the exciting source. The excitation source of homogeneous light (420 nm) was filtered from the xenon lamp (PLS-SXE300D, China).

2.3 Preparation of CuO/Cu_2O Nanowire electrode

The CuO/Cu_2O Nanowire was synthesized by simple two steps [31,32]. The first step was to prepare the $Cu(OH)_2$ naonowire array ($Cu(OH)_2$ Nanowire) on copper foam by a wet-chemistry method. A piece of copper foam (2 cm×3 cm) was carefully pre-treated by hydrochloric acid, ethanol and deionized water for several times to remove the surface oxide and impurities. Then, the clean copper foam was immersed in the 30 mL solution which contained 3.2 g of NaOH and 0.89 g of $(NH_4)_2S_2O_8$ for 20 min. The sample was taken out and rinsed several times with deionized water. Then the $Cu(OH)_2$ Nanowire was obtained. Secondly, the precursor was heated at 350 °C for 15 min in a static N_2 atmosphere, and then naturally cooled to ambient temperature under N_2. Finally, the CuO/Cu_2O Nanowire was obtained.

2.4 Fabrication of PEC biosensor for the detection of tyrosinase

The CuO/Cu_2O Nanowire (0.5 cm×0.5 cm) was decorated with amino groups by depositing 20 μL of 0.5 wt% chitosan solution (the chitosan powder was ultrasonically dissolved in 1% acetic acid and then diluted to desired concentrations by 0.1 M Tris-HCl buffer solution (pH 7.0)) and dried in room temperature. Then, the mixture containing 100 μL of 1 mM tyrosine, 100 μL of 0.1 M Tris-HCl buffer solution (pH 7.0) and 100 μL of different concentration of tyrosinase was incubated at 37 °C, and the chitosan deposited CuO/Cu_2O Nanowire was immersed in the mixture for 90 min. After that, the as-prepared electrode was taken out and washed with deionized water for several times. Finally, the working electrode was immersed in 0.1 M Tris-HCl buffer solution (pH 7.0) for PEC measurement at 0 V (vs. Ag/AgCl).

3 Results and discussion

3.1 Characterization of CuO/Cu_2O Nanowire

X-ray diffraction (XRD) was employed to characterize the compositions and phase of materials. Figure S1 displays the XRD pattern of $Cu(OH)_2$ Nanowire. The noticeable signals appeared at 16.6°, 23.7°, 33.9°, 35.5°, 38.4°, 39.80°, 43.3°, 48.7° and 53.2° are assigned to the (020), (021), (041), (111), (022), (130), (131), (042) and (150) planes of hexagonal $Cu(OH)_2$ [31]. Figure 1(a) displays the X-ray diffraction (XRD) pattern of CuO/Cu_2O Nanowire. The CuO diffraction peaks positioned at 35.2°, 38.5°, 48.6°, 66.1° and 67.8° are indexed to the (022), (111), (–202), (–331), (113) and (311) planes, respectively. In addition, the well defined peaks located at 29.5°, 36.4°, 42.3°, 61.3°, 73.5° and 77.3° correspond to diffraction of the (110), (111), (200), (220), (311) and (222) planes of Cu_2O [32]. Figure S2 shows the FTIR spectra of CuO/Cu_2O Nanowire and CuO/Cu_2O Nanowires-chitosan. The strong absorption peaks at 3373 cm^{-1}, 1603 cm^{-1} and 1443 cm^{-1} represented the amino groups in CuO/Cu_2O Nanowires-chitosan [33,34]. Figure 1(b) and 1(c) exhibit the scanning electron microscopy (SEM) images of $Cu(OH)_2$ Nanowire. It can been seen that the copper foam is covered by $Cu(OH)_2$ nanowires completely. After heat treatment at 350 °C, the morphology of CuO/Cu_2O still remained nanowire array (Figure 1(d) and 1(e)). And the high-resolution scanning electron microscopy (SEM) images of CuO/Cu_2O Nanowire demonstrated the nanowire morphology (Figure S3). Furthermore, the energy dispersive X-ray (EDX) mapping images indicate the elements of Cu and O are uniformly dispersed in the nanowire array (Figure S4). The transmission electron microscopic (TEM) was conducted to character the morphology of CuO/Cu_2O Nanowire as well. In Figure 1(f), the TEM image of CuO/Cu_2O Nanowire represents its nanowire morphology which is consistent with the SEM results. As shown in Figure 1(g), the high-resolution transmission electron microscopy (HRTEM) taken from the single nanowire shows the as-made material had two well-resolved lattice plane distances which were determined to be 0.245 nm and 0.254 nm, corresponding to the CuO (111) and Cu_2O (111) crystal planes, respectively.

The X-ray photoelectron spectroscope (XPS) analysis was used to gain more insight into the element valence state and examine chemical composition of photoelectrode. In Figure S5(A), the XPS survey spectrum confirms the presence of Cu and O elements. The peak of C element arose from CO_2 in air. In Figure 1(h), the main peaks located at 932.7 eV and

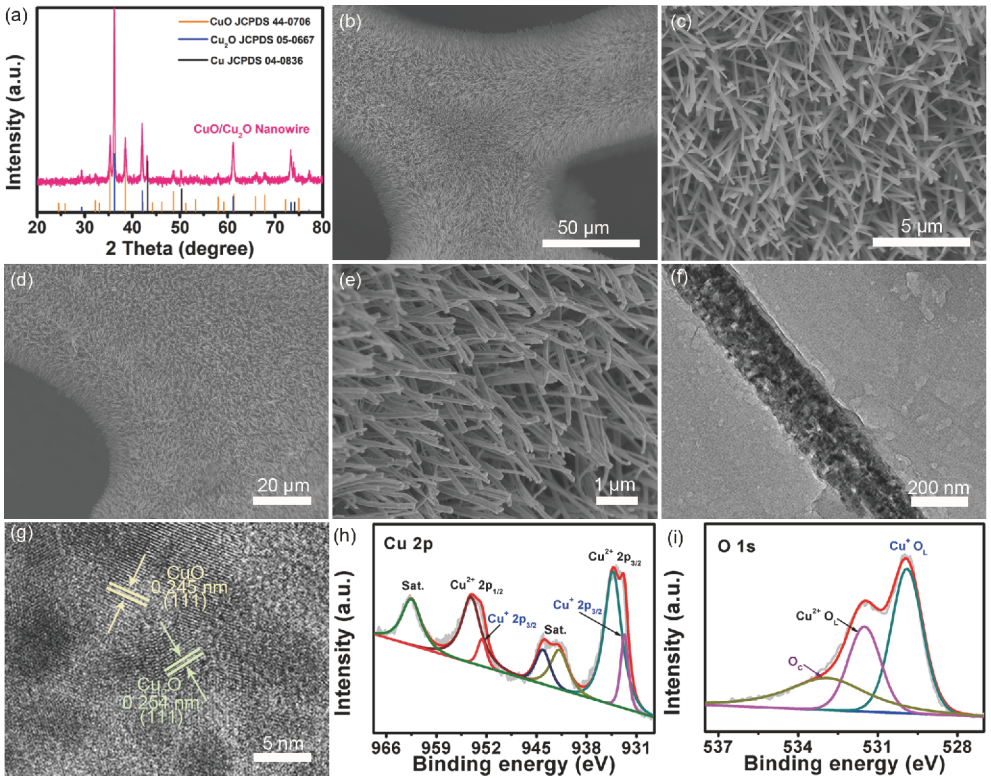

Figure 1 (a) XRD pattern of CuO/Cu_2O Nanowire. (b, c) SEM images of $Cu(OH)_2$ Nanowire. (d, e) SEM images of CuO/Cu_2O Nanowire. (f) TEM image of single CuO/Cu_2O nanowire. (g) HRTEM image of CuO/Cu_2O. (h) Cu 2p and (i) O 1s XPS spectra of CuO/Cu_2O Nanowire (color online).

952.6 eV were assigned to Cu $2p_{3/2}$ and Cu $2p_{1/2}$, respectively, which indicated the state of Cu was +1. And the shake-up satellite (Sat.) peaks positioned at 941.8 eV, 944.1 eV and 962.5 eV demonstrated the presence of Cu^{2+} [35]. However, it is difficult to clearly identify the Cu^+ and Cu^0 species because of the effect of particle size and surface coverage on the binding energy [36]. The two weak peaks obtained by deconvoluting the major peaks at the binding energies of 932.7 eV and 952.6 eV correspond to Cu^+ or Cu^0. In the Auger Cu KLL spectrum, the peaks centered at 570.0 eV and 568.1 eV were assigned to Cu^+ and Cu^0, respectively (Figure S5(B)) [37]. By combining the Figure 1 (g), Figure S5(B) as well as XRD pattern, we can conclude that such material contains ternary valence states Cu^{2+}, Cu^+ and Cu^0 (stem from copper foam). Figure 1(i) displays the O 1s region. As observed, the O 1s curve can be resolved into three components: lattice oxygen of Cu_2O and CuO (Cu^+ O_L and Cu^{2+} O_L) and adsorbed oxygen (O_C). The XPS peaks at the binding energies of 531.4 eV and 529.9 eV belong to Cu^+ O_L and Cu^{2+} O_L, respectively. And the O_C component at the binding energy of 532.9 eV is attributed to dissociated oxygen species [38].

3.2 Electrochemical impedance spectroscopy characterization of the biosensor modification process

The electrochemical impedance spectroscopy was employed to reflect the change in charge transfer resistance (R_{ct}) during the electrode surface modification [39]. With increasing the modification of the electrode, the R_{ct} was changed accordingly. And the value of R_{ct} was estimated by the semicircle diameter of Nyquist plot. The larger semicircle diameter indicated a greater R_{ct}. In Figure 2, the Nyquist plots for different electrodes were measured in Tris-HCl buffer solution (0.1 M, pH 7.0) including 5 mM $[Fe(CN)_6]^{3-/4-}$. As observed, the CuO/Cu_2O Nanowire possessed a lowest impedance value (curve a). After depositing chitosan on the electrode, the R_{ct} increased obviously owing to the fact that the chitosan impeded the redox $[Fe(CN)_6]^{3-/4-}$ probe to the surface of the electrode (curve b). It demonstrated that the CuO/Cu_2O Nanowire-chitosan electrode was successfully assembled. When the CuO/Cu_2O Nanowire-chitosan electrode immersed in 1 mM 4-benzoquinone for 1.5 h, the value of R_{ct} decreased (curve c), confirming the 4-benzoquinone can improve the conductivity. These stepwise changes of R_{ct} values implied the PEC biosensor was constructed.

3.3 Photoelectrochemical biosensor for tyrosinase detection

In Figure 3(A), the PEC responses of different modified electrodes were investigated in 0.1 M Tris-HCl (pH 7) at 0 V vs. Ag/AgCl. The CuO/Cu_2O Nanowire possessed strong photocurrent signal (curve a). And the signal showed no

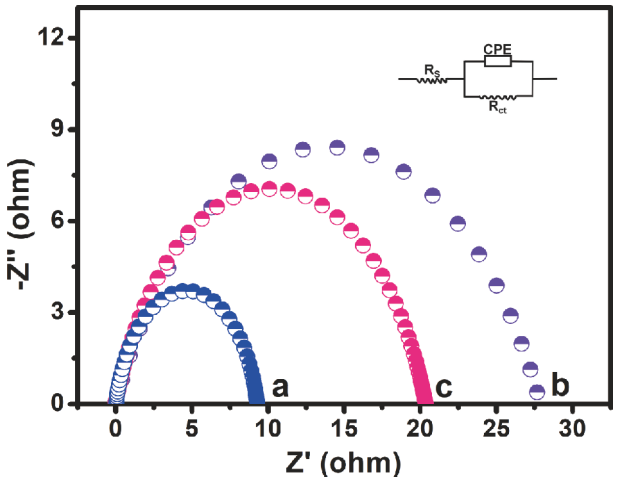

Figure 2 Nyquist plots of electrochemical impedance spectroscopy for different modified electrodes: (a) CuO/Cu_2O Nanowire, (b) CuO/Cu_2O Nanowire-chitosan, and (c) CuO/Cu_2O Nanowire-chitosan-quinones in Tris-HCl buffer solution (0.1 M, pH 7.0) including 5 mM $[Fe(CN)_6]^{3-/4-}$ (color online).

obvious change after depositing the chitosan on the electrode (curve b). When the CuO/Cu_2O Nanowire-chitosan electrode incubates with 1 mM tyrosine (curve c) and 5 U/mL tyrosinase (curve d), the photoelectric responses still showed no distinct vibration. While the CuO/Cu_2O Nanowire-chitosan incubated with 0.1 M 4-benzoquinone (curve e), the PEC response was significantly improved. In the process of illumination, the electrons both on the valence bands of Cu_2O and CuO were excited to their conductive bands resulting in the electron-hole (e^--h^+) pairs. The holes on the valence band of CuO will inject to that of Cu_2O, and then can be scavenged by the electrons generated from copper foam. In the meantime, the electrons on the conductive band of Cu_2O will transfer to that of CuO, and finally be captured by the 4-benzoquinone immobilized on the electrode. As observed in Figure S6, the CuO/Cu_2O Nanowire electrode and CuO/Cu_2O Nanowire-chitosan electrode were incubated with 0.1 M 4-benzoquinone for 1.5 h, respectively, and the latter exhibited a higher PEC response which benefited from the electron acceptor immobilized on the electrode accepting electrons quickly. These measurements demonstrated the feasibility of the proposed strategy.

As shown in Figure 3(B), the PEC change of biosensor was closely related to the concentration of tyrosinase. As the tyrosinase concentration increased from 0.05 to 10 U/mL, the photocurrent response enhanced accordingly. And each concentration sample was repeated for 5 times. The inset exhibited a good linear relationship between the change of photocurrent and the tyrosinase concentration, with a linear correlation coefficient of 0.993. In addition, on the basis of S/N=3, the calculated limit of detection was 0.016 U /mL, which was compared favorable to other reported literature for tyrosinase detection (Table S1). To obtain the optimal tyrosinase sensing performance, we investigated the effect of the tyrosinase catalytic reaction time on the photoelectric response in the range from 0.5 to 2.5 h (Figure S7). The photocurrent increased with the increase of catalytic time and then reached a summit at 1.5 h. Thus, 1.5 h was chosen as the optimized time for all the catalytic tyrosine steps of the assay.

3.4 Selectivity, reproducibility stability of the PEC biosensor

Due to the complicated conditions of practical serum samples, an efficient tyrosinase biosensor must possess superb selectivity. Some potential interfering substances such as alkaline phosphatase (ALP), bovine serum albumin (BSA), glucose oxidase (GOx), K^+, Zn^{2+}, trypsin, glucose and threonine were chosen to test the selectivity performance of the fabricated biosensor. The concentrations of ALP, GOx, trypsin threonine and tyrosinase used in this process were 5 U/L and the concentrations of K^+, Zn^{2+}, BSA and glucose were 0.1 mM. And each substance was measured in parallel five times. As shown in Figure 4, these aforementioned interferential substances display relatively low photoelectric signals compared to the photocurrent of tyrosinase. The re-

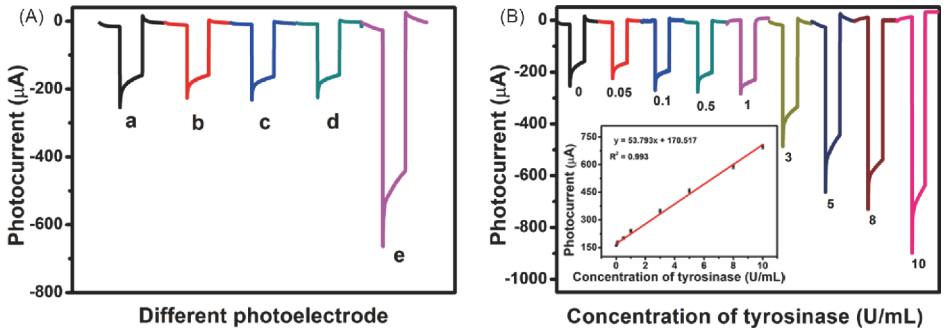

Figure 3 (A) PEC responses of (a) CuO/Cu_2O Nanowire, (b) CuO/Cu_2O Nanowire-chitosan, CuO/Cu_2O Nanowire-chitosan incubating with (c) 1 mM tyrosine, (d) 5 U/mL tyrosinase and (e) 0.1 M 4-benzoquinone for 1.5 h at 0 V vs. Ag/AgCl. (B) Photocurrent responses of the developed PEC electrode records in 0.1 M Tris-HCl (pH 7) containing 1 mM tyrosine and various concentrations of tyrosinase, and the inset is the corresponding calibration plot curve (color online).

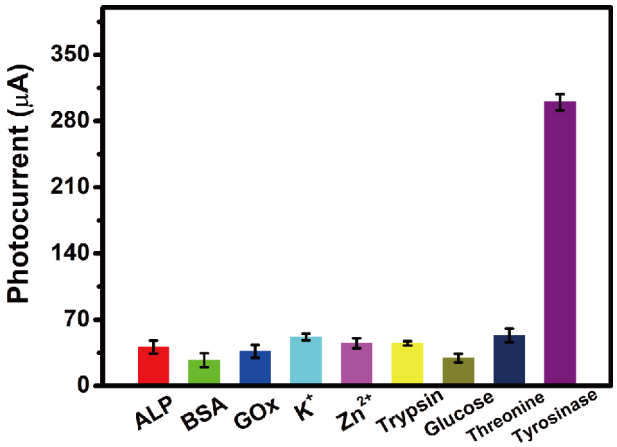

Figure 4 Selectivity of the developed platform for tyrosinase detection. The concentrations of ALP, GOx, trypsin threonine and tyrosinase were 5 U/mL and K^+, Zn^{2+}, BSA and glucose were 1 mM (color online).

sults signify that the developed platform possesses an excellent selectivity for tyrosinase. In addition, the stability of biosensor was assessed by chronopotentiometric measurement. The CuO/Cu_2O Nanowire was test for more than 800 s and repeated the illumination process for more than 20 times in Tris-HCl (0.1 M, pH 7). After long-time measurement, the photocurrent had no obvious decreased (Figure S8) which indicates a good stability of proposed biosensor.

In order to validate the feasibility of the proposed PEC biosensor, we also applied it to determine tyrosinase in human serum samples by standard addition method. As shown in Table S2, the recovery results of spiked 10-fold diluted human serum samples are summarized. The RSD was 1.6%–3.2% and the good recoveries are in range of 96% to 105%, which implied that other chemical species presented in human serum samples did not interfere with the quantification of tyrosinase and the PEC biosensor was reliable in real applications.

4 Conclusions

In summary, a CuO/Cu_2O Nanowire electrode was synthesized for tyrosinase detection by quinone-chitosan conjugation chemistry method. In the PEC process, the *in-situ* generated quinones, the electron acceptors, will be immobilized by the chitosan modified on the surface of the electrode, resulting in an obvious signal amplification. The highly sensitive PEC biosensor can realize a rapid response in a wild linear range of 0.05 U/mL to 10 U/mL with the detection limit as low as 0.016 U/mL and showed high selectivity and good stability. Such fabricated biosensor sheds light on a new methodology for tyrosinase detection, and has a great potential for clinical and biological analysis in the future.

Acknowledgements This work was supported by the National Natural Science Foundation of China (21775089), the Outstanding Youth Foundation of Shandong Province (ZR2017JL010), the Key Research and Development Program of Jining City (2018ZDGH032) and Taishan scholar of Shandong Province (tsqn201909106). Thanks eceshi (www.eceshi.cn) for XPS analysis.

Conflict of interest The authors declare that they have no conflict of interest.

Supporting information The supporting information is available online at http://chem.scichina.com and http://link.springer.com/journal/11426. The supporting materials are published as submitted, without typesetting or editing. The responsibility for scientific accuracy and content remains entirely with the authors.

1 Kim TI, Park J, Park S, Choi Y, Kim Y. *Chem Commun*, 2011, 47: 12640–12642
2 Yan X, Li H, Zheng W, Su X. *Anal Chem*, 2015, 87: 8904–8909
3 Corani A, Huijser A, Gustavsson T, Markovitsi D, Malmqvist PÅ, Pezzella A, d'Ischia M, Sundström V. *J Am Chem Soc*, 2014, 136: 11626–11635
4 Yu SY, Xue TY, Zhu LB, Fan GC, Han DM, Wang C, Zhao WW. *Biosens Bioelectron*, 2019, 136: 128–131
5 Decker H, Dillinger R, Tuczek F. *Angew Chem Int Ed*, 2000, 39: 1591–1595
6 Solem E, Tuczek F, Decker H. *Angew Chem Int Ed*, 2016, 55: 2884–2888
7 Wu X, Li X, Li H, Shi W, Ma H. *Chem Commun*, 2017, 53: 2443–2446
8 Huang FW, Hodis E, Xu MJ, Kryukov GV, Chin L, Garraway LA. *Science*, 2013, 339: 957–959
9 Davies H, Bignell GR, Cox C, Stephens P, Edkins S, Clegg S, Teague J, Woffendin H, Garnett MJ, Bottomley W, Davis N, Dicks E, Ewing R, Floyd Y, Gray K, Hall S, Hawes R, Hughes J, Kosmidou V, Menzies A, Mould C, Parker A, Stevens C, Watt S, Hooper S, Wilson R, Jayatilake H, Gusterson BA, Cooper C, Shipley J, Hargrave D, Pritchard-Jones K, Maitland N, Chenevix-Trench G, Riggins GJ, Bigner DD, Palmieri G, Cossu A, Flanagan A, Nicholson A, Ho JWC, Leung SY, Yuen ST, Weber BL, Seigler HF, Darrow TL, Paterson H, Marais R, Marshall CJ, Wooster R, Stratton MR, Futreal PA. *Nature*, 2002, 417: 949–954
10 Zhan C, Cheng J, Li B, Huang S, Zeng F, Wu S. *Anal Chem*, 2018, 90: 8807–8815
11 Teng Y, Jia X, Li J, Wang E. *Anal Chem*, 2015, 87: 4897–4902
12 Wei J, Qiu J, Li L, Ren L, Zhang X, Chaudhuri J, Wang S. *Nanotechnology*, 2012, 23: 335707
13 Liu JW, Wang YM, Xu L, Duan LY, Tang H, Yu RQ, Jiang JH. *Anal Chem*, 2016, 88: 8355–8358
14 Khoobi A, Ghoreishi SM, Behpour M, Masoum S. *Anal Chem*, 2014, 86: 8967–8973
15 Salamon J, Sathishkumar Y, Ramachandran K, Lee YS, Yoo DJ, Kim AR, Gnana Kumar G. *Biosens Bioelectron*, 2015, 64: 269–276
16 Lei C, Zhao XE, Sun J, Yan X, Gao Y, Gao H, Zhu S, Wang H. *Talanta*, 2017, 175: 457–462
17 Lin Y, Yin M, Pu F, Ren J, Qu X. *Small*, 2011, 7: 1557–1561
18 Zhao WW, Ma ZY, Yan DY, Xu JJ, Chen HY. *Anal Chem*, 2012, 84: 10518–10521
19 Wang GL, Shu JX, Dong YM, Wu XM, Li ZJ. *Biosens Bioelectron*, 2015, 66: 283–289
20 Izaki M, Fukazawa K, Sato K, Khoo PL, Kobayashi M, Takeuchi A, Uesugi K. *ACS Appl Energy Mater*, 2019, 2: 4833–4840
21 Liu X, Chen J, Liu P, Zhang H, Li G, An T, Zhao H. *Appl Catal A-General*, 2016, 521: 34–41
22 Baghriche O, Rtimi S, Pulgarin C, Kiwi J. *Catal Today*, 2017, 284:

77–83
23 Wu HW, Lee SY, Lu WC, Chang KS. *Appl Surf Sci*, 2015, 334: 236–241
24 Li B, Lai C, Zeng G, Qin L, Yi H, Huang D, Zhou C, Liu X, Cheng M, Xu P, Zhang C, Huang F, Liu S. *ACS Appl Mater Interfaces*, 2018, 10: 18824–18836
25 Wei Z, Benlin D, Fengxia Z, Xinyue T, Jiming X, Lili Z, Shiyin L, Leung DYC, Sun C. *Appl Catal B-Environ*, 2018, 229: 171–180
26 Liu YL, Zhu YC, Qu LB, Yang R, Yu XD, Zhao WW. *ACS Appl Bio Mater*, 2019, 2: 2703–2707
27 Guo X, Liu S, Yang M, Du H, Qu F. *Biosens Bioelectron*, 2019, 139: 111312–111318
28 Guo X, Kong RM, Zhang X, Du H, Qu F. *ACS Catal*, 2018, 8: 651–655
29 Wang GL, Yuan F, Gu T, Dong Y, Wang Q, Zhao WW. *Anal Chem*, 2018, 90: 1492–1497
30 Kumar G, Smith PJ, Payne GF. *Biotechnol Bioeng*, 1999, 63: 154–165
31 Xie L, Tang C, Wang K, Du G, Asiri AM, Sun X. *Small*, 2017, 13: 1602755
32 Liu J, Wang L, Wang N, Guo F, Hou L, Chen Y, Liu J, Zhao Y, Jiang L. *Small*, 2016, 13: 1600499
33 Jiang D, Xue J, Wu L, Zhou W, Zhang Y, Li X. *Appl Catal B-Environ*, 2017, 211: 199–204
34 Yusof NAA, Zain NM, Pauzi N. *International Journal of Biological Macromolecules*, 2019, 124: 1132–1136
35 Lin S, Liu L, Yang Y, Lin K. *Appl Surf Sci*, 2017, 407: 29–35
36 Dubale AA, Pan CJ, Tamirat AG, Chen HM, Su WN, Chen CH, Rick J, Ayele DW, Aragaw BA, Lee JF, Yang YW, Hwang BJ. *J Mater Chem A*, 2015, 3: 12482–12499
37 Li J, Zhang Z, Ji Y, Jin Z, Zou S, Zhong Z, Su F. *Nano Res*, 2016, 9: 1377–1392
38 Platzman I, Brener R, Haick H, Tannenbaum R. *J Phys Chem C*, 2008, 112: 1101–1108
39 Wang Y, Lü Y, Zhan W, Xie Z, Kuang Q, Zheng L. *J Mater Chem A*, 2015, 3: 12796–12803
40 Chen J, Zhao GC. *Biosens Bioelectron*, 2017, 98: 155–160